

⁹L. A. Charlton, J. M. Eisenberg, and A. B. Jones, Nucl. Phys. **A71**, 625 (1971).

¹⁰C. W. Wilkin, CERN Report No. CERN 71-74 (unpublished), 365-366.

¹¹N. Auerbach and J. Warszawski, Phys. Lett. **45B**, 171 (1973).

¹²D. Tow and J. M. Eisenberg, Nucl. Phys. **A237**, 441 (1975).

¹³B. J. Dropesky, G. W. Butler, C. J. Orth, R. A. Williams, G. Friedlander, M. A. Yates, and S. Kaufmann, Phys. Rev. Lett. **34**, 821 (1975).

¹⁴M. E. Bellotti, D. Cavalli, and C. Matteuzzi, Nuovo Cimento A **18**, 75 (1973).

¹⁵C. Wong, J. D. Anderson, S. D. Bloom, J. M. McClure, and B. D. Walker, Phys. Rev. **123**, 598 (1966); C. J. Batty, B. E. Bonner, E. Friedman, C. Tshalar, L. E. Williams, A. S. Clough, and J. B. Hunt, Nucl. Phys. **A120**, 297 (1968); R. R. Borchers and C. H. Pope, Phys. Rev. **129**, 2679 (1963); S. A. Elbaker, I. J.

Heerden, W. J. McDonald, and G. C. Neilson, Nucl. Instrum. Methods **105**, 519 (1972); L. Valentin, Nucl. Phys. **62**, 81 (1964).

¹⁶F. Ajzenberg-Selove and T. Lauritsen, Nucl. Phys. **A227**, 1 (1974).

¹⁷W. R. Gibbs, private communication.

¹⁸L. C. Liu and W. Franco, in Proceedings of the Sixth International Conference on High Energy Physics and Nuclear Structure, Santa Fe, New Mexico, 1975 (to be published); W. R. Gibbs, B. F. Gibson, A. I. Hess, G. J. Stephenson, Jr., and W. B. Kaufmann, *ibid.*;

T. S. H. Lee, K. Kubonderan, and J. D. Vergados, *ibid.*

¹⁹W. R. Gibbs, B. F. Gibson, A. T. Hess, G. J. Stephenson, Jr., and W. B. Kaufmann, to be published; J. M. Eisenberg and A. Gal, to be published; L. C. Liu and V. Franco, to be published; and G. A. Miller and J. E. Spencer, to be published.

²⁰N. Auerbach and J. Warszawski, private communication.

Pion Charge-Exchange Scattering from Light Nuclei*

W. R. Gibbs, B. F. Gibson, A. T. Hess, and G. J. Stephenson, Jr.

Theoretical Division, Los Alamos Scientific Laboratory, University of California, Los Alamos, New Mexico 87545

and

W. B. Kaufmann

Arizona State University, Tempe, Arizona 85281

(Received 11 September 1975)

The reactions ${}^7\text{Li}(\pi^+, \pi^0){}^7\text{Be}$, ${}^{10}\text{B}(\pi^+, \pi^0){}^{10}\text{C}$, and ${}^{13}\text{C}(\pi^+, \pi^0){}^{13}\text{N}$ are examined using a full multiple-scattering formalism with a separable form assumed for the pion-nucleon t matrix. Spin-flip contributions are included. We find that the contributions arising from transitions to nonanalog final states in the case of ${}^{10}\text{B}$ and ${}^7\text{Li}$ are of the same order of magnitude as pure analog cross sections.

Pion-nucleus charge-exchange scattering has been studied as a means of probing nuclear structure details. Early theoretical works on this problem have used either optical models in a coupled-channel or distorted-wave formalism,¹ or multiple-scattering expansions, such as Glauber theory.² However, from the results of such calculations, it seems that those optical models incorporate too much absorption. The validity of applying the Glauber theory to pion-nucleus charge exchange is questionable, considering the lack of forward peaking in the pion-nucleon charge-exchange amplitudes contrary to a Glauber-theory assumption.

We have used a fixed-nucleon, full multiple-scattering treatment³ free from the approximations of optical models and also free of the small-angle forward-peaked assumptions of Glauber theory. The basic features of the formalism are

described by Gibbs, Jackson, and Kaufmann.⁴

Here we use a separable form for the pion-nucleon t matrix,⁵ instead of the pole approximation used there. This enables us to treat the off-shell properties of the pion-nucleon scattering more realistically. The t matrix used has the form

$$\langle \vec{q} | t(\omega) | \vec{q}' \rangle = \lambda_0(\omega) V_0(q) V_0(q') + \lambda_1(\omega) \vec{q} \cdot \vec{q}' V_1(q) V_1(q'), \quad (1)$$

where

$$\omega = (k^2 + \mu^2)^{1/2}$$

and

$$V_i(q) = \frac{k^2 + \alpha_i^2}{q^2 + \alpha_i^2}, \quad \lambda_i(\omega) = \frac{\exp[2i\delta_i(\omega)] - 1}{k^{2i+1}}. \quad (2)$$

The parameters α_i have been determined by fits

to π -deuteron absorption: $\alpha_0 = 500$ MeV/c and $\alpha_1 = 300$ MeV/c.

The set of multiple-scattering equations which we must solve can be written in the shorthand form

$$G_i = f_i + f_i \sum_{j \neq i} G_j, \quad (3)$$

where the first term on the right-hand side represents single scattering and the second describes multiple scattering to all orders, the last scattering being on the i th nucleon. The quantity f_i is the pion-nucleon scattering amplitude, and G_i is related to the pion-nucleus scattering amplitude by

$$F(\vec{k}, \vec{k}') = \sum G_i(\vec{k}, \vec{k}') \exp(-i\vec{k}' \cdot \vec{r}_i).$$

This amplitude must then be averaged over the appropriate nuclear wave functions. By allowing for charge exchange, we can formulate a set of coupled equations, similar in form to Eq. (3), but containing amplitudes for charge-exchange as well as elastic scattering. Matrix techniques can then be used in the fixed-nucleon approximation to solve for the total charge-exchange amplitude.⁴

For the charge-exchange reactions which we consider, some transitions are to nonanalog final states. We account for this by constructing models which describe such states. In addition, we examine the multipole structure of the probed nuclear density by writing the charge-exchange transition operator as $\sum \hat{\Theta}_i(r_1, \dots, r_A) \tau_i^+$, where $\hat{\Theta}$ is a full A -particle multiple-scattering operator and τ_i^+ is the isospin-raising operator. Making use of the antisymmetrization properties of our wave functions and using standard angular-momentum techniques enable us to combine spherical harmonics of the valence nucleons from initial and final states and thus project out the appropriate (even) multipoles of the nuclear form factor. The coefficients of these higher multipole terms are then used in the full multiple-scattering calculation.

We calculate the (π^+ , π^0) cross sections to particle-stable states for ^{10}B , ^7Li , and ^{13}C for pion energies ranging from 20 to 260 MeV. Harmonic-oscillator densities are used. The results are compared to the data of Shamai *et al.*⁶

For ^{10}B , we use a model consisting of two nucleons outside a ^8Be core, coupled to the appropriate total angular momentum with space symmetry components chosen to mock up shell-model results.⁷ The initial state is 3^+ and there are

two particle-stable final states in the residual ^{10}C , the 0^+ ground state and the 2^+ 3.34-MeV state, both reached by nonanalog transitions. The transition from 3^+ to 0^+ must go by quadrupole spin flip, whereas the 3^+ to 2^+ transition can proceed by either monopole or quadrupole. Figure 1 shows the summed cross section to both final states for two choices of the oscillator parameter, b . For $b = 1.6$ fm (the value indicated by electron scattering) we also display the monopole and quadrupole components of the cross section. For energies above 50 MeV, the quadrupole transition strongly dominates. The transition to the 2^+ state is the larger, being approximately an order of magnitude greater than the transition to the 0^+ state throughout the energy range. For energies up to 80 MeV, spin-flip and spin-nonflip parts are comparable. From 80 to 200 MeV, spin-flip dominates, and above 200 MeV, the spin-nonflip cross section is larger.

For ^7Li , the initial state is $\frac{3}{2}^-$. There are two particle-stable final states: the $\frac{3}{2}^-$ analog and the $\frac{1}{2}^-$ first excited state. Hence both monopole and quadrupole transitions are allowed to either final state when spin flip is included. To describe the mass-7 nuclei, we use a full shell-model treatment⁸ which considers three nucleons

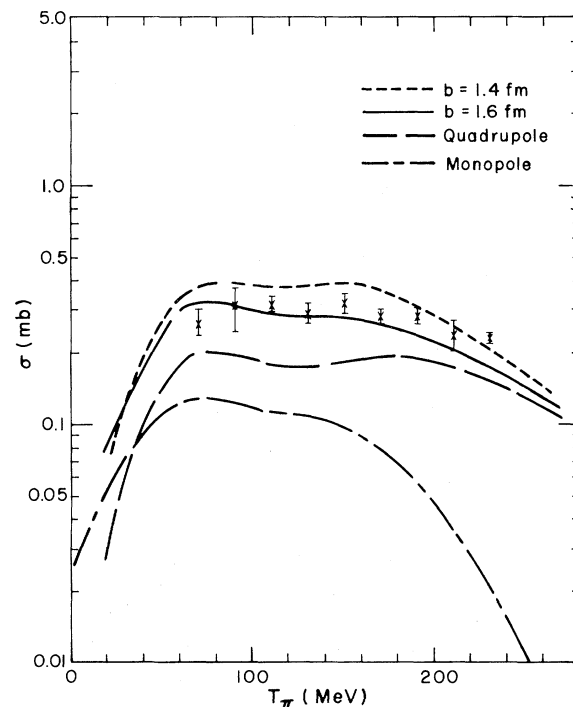
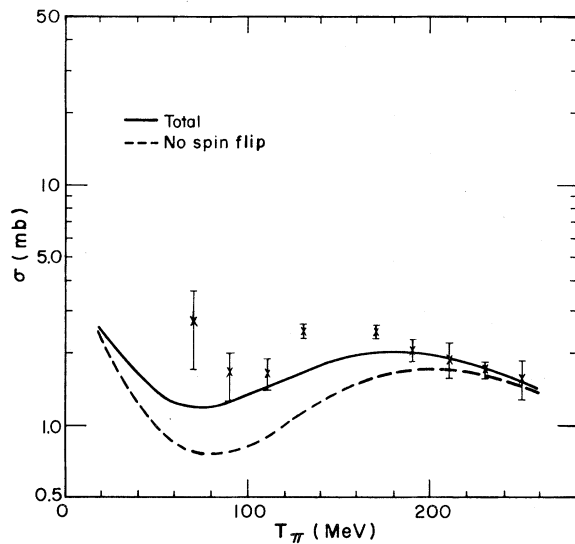


FIG. 1. Cross section for ^{10}B . Monopole and quadrupole curves have $b = 1.6$ fm.

FIG. 2. Cross section for ${}^7\text{Li}$.

outside an α -particle core. The results of the calculation are shown in Fig. 2. The curves shown are the summed cross sections to both final states and contain both monopole and quadrupole components. The cross sections to each of the two final states are of comparable size. The effect of including spin-flip transitions can be clearly seen.

We also examine the reaction ${}^{13}\text{C}(\pi^+, \pi^0){}^{13}\text{N}$. This is a pure analog transition, with $\frac{1}{2}^-$ initial and final states, and proceeds entirely via the monopole form factor. In Fig. 3 we show our result including spin flip. Various modifications were studied including deformation of the ${}^{13}\text{C}$ nucleus⁹ and antisymmetrization of the p -shell nucleons. These modifications do not significantly lessen the discrepancy with the data. Different parametrizations of the pion-nucleon phase shifts¹⁰ give changes of about 10% for the low-energy cross sections.

Excellent agreement is obtained for the purely nonanalog ${}^{10}\text{B}$ reaction. The agreement is not as good for the two cases involving analog transitions.

Since the data are obtained by activation measurements, a process which can contribute to the discrepancy in the analog cases is nucleon charge exchange by low-energy protons produced in the target. A correction for this effect was made in Ref. 6. Our estimates of this process are energy dependent and give corrections possibly as large as 0.5 mb for ${}^{13}\text{C}$ and 1.0 mb for ${}^7\text{Li}$.¹¹ For the nonanalog ${}^{10}\text{B}$ reaction, the basic

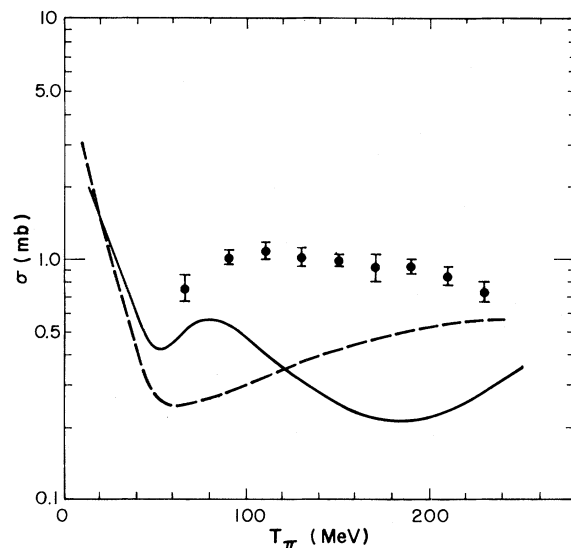


FIG. 3. Cross section for ${}^{13}\text{C}$. The solid curve is computed with a Gaussian density with $b = 1.64$ fm; the dashed curve with the "exponential tail" density of Ref. 4 with a matching radius of 3.0 fm.

(p, n) cross section is about two orders of magnitude smaller than these analog transitions, and hence this effect is negligible. Because of the difficulty of making reliable calculations of secondary production, a final comparison of theory and experiment for analog transitions must await the higher pion fluxes required for thin-target measurements or the direct detection of the final π^0 .

The fact that the ${}^{10}\text{B}$ cross section is calculated to be of the same magnitude as the analog transitions indicates that, unlike (p, n) reactions, (π^+, π^0) reactions do not select analog transitions. This results because the basic $\pi^+ - n$ charge-exchange amplitude is substantial at large angles, leading to good overlap with higher transition multipole moments. This feature has significance for the $(\pi^+, \pi^0\bar{p})$ experiments, as there should be an appreciable \bar{p} production from non-analog states.¹²

*Work supported in part by the U. S. Energy Research and Development Administration.

¹L. A. Charlton, J. M. Eisenberg, and W. B. Jones, Nucl. Phys. **A171**, 625 (1971); E. Rost and G. W. Edwards, Phys. Lett. **37B**, 247 (1971); G. E. Miller and J. E. Spencer, Phys. Lett. **53B**, 329 (1974); M. Koren, Ph.D. thesis, Massachusetts Institute of Technology, 1969 (unpublished); D. Tow and J. M. Eisenberg, Nucl. Phys. **A237**, 441 (1975).

²M. A. Locchi and P. Picchi, *Nuovo Cimento* **57**, 803 (1968); A. Reitan, *Nucl. Phys.* **B68**, 387 (1974).

³W. R. Gibbs, *Phys. Rev. C* **3**, 1127 (1971), and **5**, 775 (1972).

⁴W. R. Gibbs, J. C. Jackson, and W. B. Kaufmann, *Phys. Rev. C* **9**, 1340 (1974).

⁵L. L. Foldy and J. D. Walecka, *Ann. Phys. (N.Y.)* **54**, 447 (1969); R. H. Landau and F. Tabakin, *Phys. Rev. D* **5**, 2746 (1972); W. R. Gibbs, *Phys. Rev. C* **10**, 2166 (1974); J. T. Londergan, K. W. McVoy, and E. J. Moniz, *Ann. Phys. (N.Y.)* **86**, 147 (1974).

⁶Y. Shamaï *et al.*, preceding Letter [*Phys. Rev. Lett.* **36**, 82 (1976)].

⁷A. N. Boyarkina, *Izv. Akad. Nauk SSSR, Ser. Fiz.* **28**, 337 (1964) [*Bull. Acad. Sci. USSR, Phys. Ser.* **28**, 255 (1964)].

⁸F. C. Barker, *Nucl. Phys.* **83**, 418 (1966).

⁹N. E. Reid, G. J. Stephenson, Jr., and M. K. Banerjee, *Phys. Rev. C* **5**, 287 (1972).

¹⁰J. M. McKinley, *Rev. Mod. Phys.* **35**, 788 (1963); L. D. Roper, R. M. Wright, and B. T. Feld, *Phys. Rev.* **138**, B190 (1965); J. R. Carter, D. V. Bugg, and A. A. Carter, *Nucl. Phys.* **B58**, 378 (1973); D. Dodder, private communication.

¹¹A group at the University of Colorado has done an independent estimate for ¹³C and obtain results similar to ours. R. E. Anderson, J. J. Kraushaar, E. Rost, and D. A. Sparrow, private communication.

¹²A. I. Yavin, R. A. Hoffswell, L. H. Jones, and T. M. Noweir, *Phys. Rev. Lett.* **23**, 1049 (1966); J. Alster, D. Ashery, A. I. Yavin, J. Duclos, J. Miller, and M. A. Moinester, *Phys. Rev. Lett.* **28**, 313 (1972); J. S. Lilley, D. H. Fitzgerald, C. H. Poppe, S. M. Grimes, and C. Wong, *Bull. Am. Phys. Soc.* **20**, 628 (1975).

Possibility of Detecting Density Isomers in High-Density Nuclear Mach Shock Waves*

Jürgen Hofmann, Horst Stöcker, Ulrich Heinz, Werner Scheid, and Walter Greiner
Institut für Theoretische Physik der Universität Frankfurt am Main, Frankfurt am Main, Germany

(Received 29 September 1975)

Up to now no experimentally feasible method for detecting abnormal nuclear states has been known. We propose to observe them in high-energy heavy-ion collisions through the disappearance of, or irregularities in, high-density nuclear Mach shock phenomena.

Even though nuclear density isomers were suggested recently by several authors,¹⁻⁵ there has been up to now no known experimentally feasible way for their detection. We suggest here a rather simple and unique method for their observation, which is based on high-density nuclear Mach shock (HDNMS) waves and head shock waves occurring during the interpenetration of high-energy heavy ions.⁶⁻⁸ Indeed, the recent experiments of Baumgardt *et al.*⁸ could be consistently interpreted with the shock-wave concept. In particular, these experiments lead to the conclusion that the observed Mach angles cannot be explained with simple sound waves of low amplitude⁹ close to nuclear equilibrium density ρ_0 but that HDNMS waves are necessary for which the actual density ρ/ρ_0 is approximately 3-6. At these densities isomeric or abnormal nuclear states may exist¹⁻⁵ which will affect the properties of the nuclear system. The situation can schematically be represented by the compression-energy functional $W_c(\rho)$ [Fig. 1(a)]. Its first minimum is associated with the nuclear ground state of binding energy $M_0c^2 - W_0 \approx 16$ MeV, and its second minimum, separated by a barrier from the first one, represents the density isomer. This secondary

minimum and particularly the binding energy $M_0c^2 - W_2$ of abnormal nuclear matter may shift up or down by a few hundred MeV.¹⁻⁵ Moreover, the compression energy of the isomer, which is determined by the compression constant $K_2 = 9\rho_2^2 \times d^2W/d\rho_2^2$ of the second minimum, may drastically deviate from that of the ground state ($K_0 \approx 300$ MeV)⁸ and lead to very high sound velocities in abnormal nuclear matter $c_s/c = (\partial p/\partial e)^{1/2}$ at constant entropy, where $e = W\rho$ is the energy density and $p = \rho^2 \partial W/\partial \rho$ is the pressure. Requiring the conservation of flux of baryons, energy, and momentum across the shock front one gets the relativistic Rankine-Hugoniot (RRH) equation

$$\frac{i_0^2}{\rho_0^2} - \frac{i^2}{\rho^2} + p \left(\frac{i_0}{\rho_0^2} + \frac{i}{\rho^2} \right) = 0 \quad (1)$$

which uniquely connects the specific enthalpies $i = W\rho + p$ and $i_0 = W_0\rho_0$ ($p_0 = 0$), the pressure p , and the densities ρ and ρ_0 on the two sides of the shock front. The index zero denotes the unshocked nuclear matter. For the energy per baryon $W(\rho, T)$ in compressed nuclear matter we made the following *Ansatz*:

$$W(\rho, T) = M_0c^2 + W_c(\rho) + W_T(\rho, T), \quad (2)$$